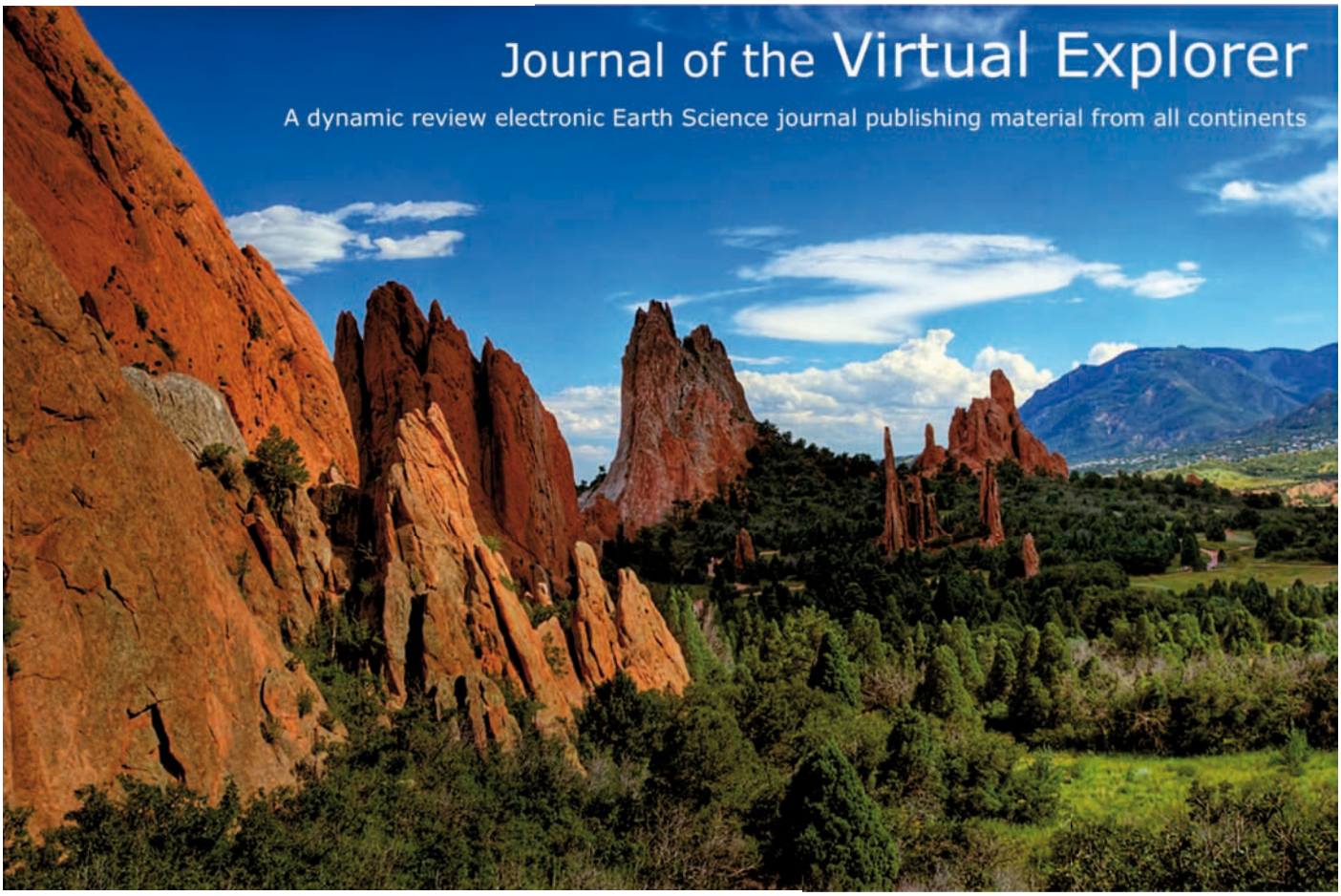

Melt inclusions in migmatites and granulites

Bernardo Cesare, Antonio Acosta-Vigil, Silvio Ferrero, Omar Bartoli

Journal of the Virtual Explorer, Electronic Edition, ISSN 1441-8142, volume **38**, paper 2
In: (Eds.) Marnie A. Forster and John D. Fitz Gerald,
The Science of Microstructure - Part II, 2011.

Journal of the Virtual Explorer, 2011
Volume 38
Paper 2
http://virtualexplorer.com.au/

Melt inclusions in migmatites and granulites

Bernardo Cesare
Department of Geosciences, University of Padova, Italy. *Email: bernardo.cesare@unipd.it*

Antonio Acosta-Vigil
Instituto Andaluz de Ciencias de la Tierra, CSIC-Universidad de Granada, Granada, Spain

Silvio Ferrero
Department of Geosciences, University of Padova, Italy.

Omar Bartoli
Dipartimento di Scienze della Terra, Università di Parma, Parma, Italy

Abstract: Important advances have been made during the last 15 years in the study of melt inclusions in minerals from migmatites and granulites. Pioneer work on high temperature metapelitic anatectic enclaves in peraluminous dacites from SE Spain has shown that droplets of granitic melt can be trapped by minerals growing during incongruent melting reactions, and that the composition of such trapped melts can be representative of that of the bulk melt in the system during the anatexis of the rock. Therefore melt inclusions may represent samples of embryionic anatectic granite. In most cases, these melt inclusions define microstructures that are typical of primary entrapment, and show little or no evidence of melt crystallization upon cooling. Rather, the melt solidified to glass due to very fast cooling associated with the submarine extrusion of the dacites. Hence inclusions can readily be analyzed for major and trace elements by conventional methods such as the electron microprobe or by laser ablation-inductively coupled plasma-mass spectrometry.

Based on the results from these quite unusual anatectic enclaves, one would expect similar melt inclusions to be present also in more conventional, slowly cooled, regionally metamorphosed migmatite and granulite terranes. As a matter of fact, recent investigations confirm this hypothesis. Tiny (<25 μm) inclusions containing a cryptocrystalline aggregate of quartz, feldpars, biotite and muscovite have been found in garnet from the metapelitic granulites of the Keraka Khondalite Belt, as well as in garnet and ilmenite from metapelitic and quartzo-feldspathic migmatites from the Alps, Ronda and the Himalayas. Due to the grain-size, texture and chemical/mineralogical composition, these inclusions are called "nanogranites" and are interpreted to represent a crystallized inclusion of anatectic melt. Exceptionally and spatially associated with the nanogranites, inclusions containing glass have also been observed. In general, the preparation of the samples and analysis of these inclusions in migmatites and granulites require more sophisticated techniques than those applied to inclusions in xenoliths and enclaves, but the information on the composition of crustal anatectic melts can also be obtained.

Since its discovery, new occurrences of nanogranite are being reported, or can be inferred from re-assessment of literature data, from migmatites and granulites worldwide. These former melt inclusions open new perspectives both for the microstructural approach to partially melted rocks and for the chemical characterization of natural crustal melts.

Citation: 2011. Melt inclusions in migmatites and granulites. In: (Eds.) Marnie A. Forster and John D. Fitz Gerald, *Journal of the Virtual Explorer*, volume **38**, paper 2, doi: 10.3809/jvirtex.2011.00268

Introduction

The microstructural analysis of (former) partially melted rocks has a long history (reviewed by Vernon, 2004 and Sawyer, 2008) and has been particularly focused on the crystallization of igneous rocks (e.g., Vernon, 2010, 2011) and on the relationships between crystallization and deformation of cooling magmas or partially solidified igneous rocks (e.g., Vernon 1999; Holness, 2010). Melting and crystallization have also been investigated by experimental approaches, using both natural samples (e.g., Mehnert *et al.*, 1973; Büsch *et al.*, 1974; Fenn, 1977) and synthetic analogue materials (e.g., Means, 1989, Means and Park, 1994). However, the microstructural aspects of partial melting that can be observed in the common source rocks of granites (i.e., migmatites and granulites), and especially in the residual rock domains that are left after melt extraction (e.g., melanosomes), have only become a subject of research during the last three decades. This is due in part to the intrinsic difficulty of studying systems where the melt phase is not present anymore, and where the post-melting history may have overprinted part of, or all the indications of its former presence. Along with reaction textures that are indicative of melting, the microstructural evidence of melt in migmatites has been mainly studied, and looked for, in the intergranular melt films, layers and pools that characterize an anatectic system (see the recent reviews by Sawyer, 2008, Holness *et al.*, 2011 and Vernon 2011). More recently, a new object of study – melt inclusions - is gaining attention as a way of complementing the more traditional and well-established approaches.

In this contribution we review the main outcomes of almost 15 years of research on melt inclusions in anatectic rocks, and discuss the main outlooks, describing first the glass inclusions in minerals from enclaves in peraluminous felsic lavas, and then the melt inclusions and nanogranites in garnet and other peritectic minerals from regional migmatites and granulites. Their very small size (<25 μm) has probably caused inclusions to go almost unnoticed in the past, but nowadays the spatial resolution of imaging and analytical tools makes their characterization possible in terms of both microstructures and composition.

Although the bulk chemical composition of the melt inclusions is of paramount importance because they probably represent the best examples of anatectic melts occurring in Nature, the paper is focused mainly on the microstructural aspects, the main topic of this Special Volume. In this sense it represents an expansion of the concepts presented in Cesare (2008).

Melt inclusions in minerals

Melt inclusions (MI) are small droplets of silicate liquid trapped in minerals called *hosts*, that either quenched as glass or crystallized to a polycrystalline aggregate upon cooling of the system. Pioneered by Sorby (1858), their microstructural study has developed under the more comprehensive framework of "fluid inclusions", a category that encompasses all types of fluids regardless of their composition and density (Hollister & Crawford, 1981; Roedder, 1984). From a genetic viewpoint, a distinction can be made between inclusions that are trapped during (termed *primary*) or after (termed *secondary*) the crystallization of the host mineral. Much of the microstructural investigation of fluid inclusions (see criteria in Roedder, 1984, or Goldstein, 2003) is aimed at evaluating this important difference. Primary inclusions can provide much more petrological information, because the presence of a particular fluid can be linked to that of a particular mineral or assemblage. Here we essentially describe and discuss primary inclusions, where such origin has been constrained on the basis of one of the most robust textural criteria, named the "zonal arrangement" (Sobolev & Kostyuk, 1975): inclusions are distributed in the core of, or in annuli within, the host (Figure 1). When inclusions present *systematically* (i.e., in a comparatively large, coherent number of occurrences) a zonal arrangement, one can conclude that they most likely formed during the growth of their host. Considering MI, primary entrapment indicates the growth of a crystal in the presence of a melt phase. One of the most common processes for this to happen is the crystallization of magma, and this is the reason why MI are so important for, and so extensively studied in, igneous petrology (Clocchiatti, 1975; Frezzotti, 2001; Schiano, 2003; Webster, 2006). Melt inclusion-rich phenocrysts in lavas are typical examples of this mode of occurrence, where the host is crystallizing *from* the melt that it is being entrapped (Figure 2). A second major, and perhaps less recognized process by which MI can form, more relevant to crustal anatexis, is when the mineral host and melt form at the same time, with the host being able to trap the melt that it is growing *with*.

This circumstance takes place during incongruent melting reactions, where peritectic solid phases are

Figure 1. Microstructures indicating primary entrapment of MI

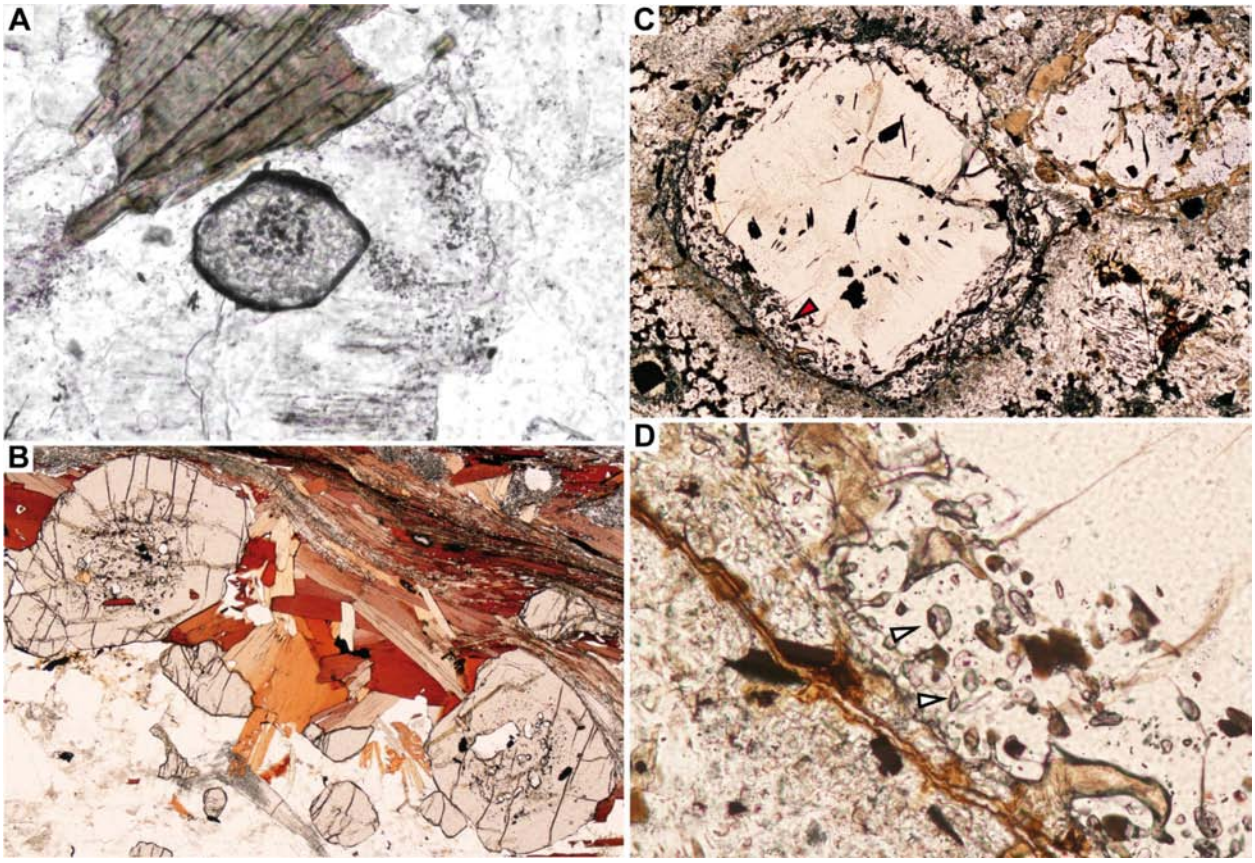

Zonal arrangement of primary MI in garnet from migmatites of Ronda (A), from the kinzigites of the Ivrea Zone (B) and from a residual enclave in the Crd-bearing rhyolites of Lipari (C and area indicated by red arrow enlarged in D, where arrows point to glassy inclusions). Widths of view: 0.35, 8.4, 3.4 and 0.42 mm, respectively.

formed together with an anatectic melt. For example, during the partial melting of metasedimentary protoliths at mid- to deep-crustal depths (0.5 - 1 GPa), the largest volumes of melt are produced by the incongruent breakdown of biotite to form peritectic garnet. Under these conditions, primary MI can be trapped in a peritectic host such as garnet (or orthopyroxene in Al_2SiO_5-free rocks).

There is a fundamental difference between the two processes of primary MI entrapment described above (i.e., melt crystallization vs. incongruent melting) , that can be visualized in the schematic representation of Figure 3, where melting and crystallization are considered essentially a function of temperature. Assuming the evolution of a partially melted system as a heating-cooling path, it can be recognized that most of the melt production by incongruent melting reactions occurs during the prograde up-T part, whereas most of melt consumption (by magma crystallization or by retrograde reactions) occurs during the down-T section. As a consequence, we

Figure 2. Primary MI in a plagioclase glomerocryst in a Crd-bearing rhyolite from San Vincenzo, Italy

The MI, arranged in concentric zones attesting to the progressive growth of the host, contain the melt that was evolving during magma crystallization. Width of view: 3.4 mm.

expect a quasi-systematic distribution of MI associated with each of these two modes of entrapment, so that MI formed during melt/magma crystallization are generally trapped during the cooling path (1 in Figure 3) and will be hosted in minerals from leucosomes or igneous rocks, whereas MI related to the melting process are mostly formed during the heating path and will be hosted in peritectic minerals (2 in Figure 3).

Figure 3. Schematic temperature (T)-time (t) diagram

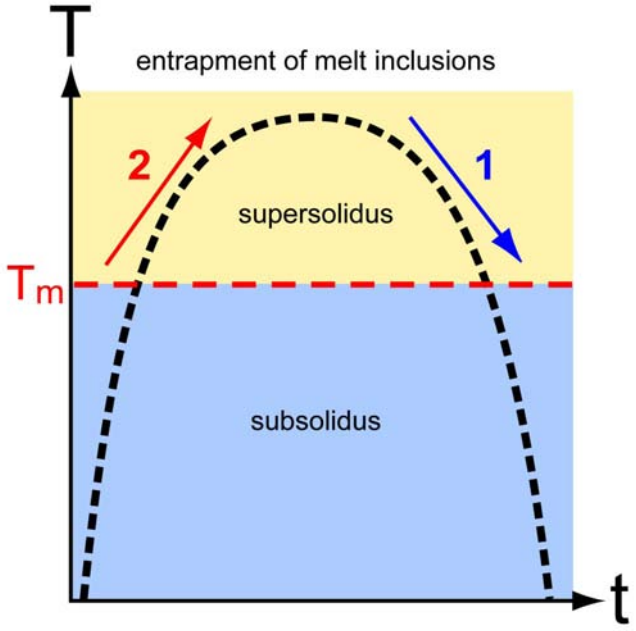

Schematic temperature (T)-time (t) diagram illustrating the two main modes of entrapment of MI during crustal anatexis and melt production (path 2), and magma crystallization (path 1). The former occurs mostly during he heating path of the rock, whereas the latter occurs dooring cooling. Only inclusions trapped along path 2 may contain primary compositions of anatectic melts.

In other words, the two modes are linked to two different parts of the evolution of an anatectic/igneous system. From a geochemical point of view this behaviour has one major consequence in that while MI in igneous rocks (including leucosomes in migmatites) contain evolved compositions, those in peritectic minerals in migmatites and granulites should display the primary compositions of anatectic melts. Although the scenario simplified in Figure 3 does not reflect the complexity of the natural processes, where pressure and composition changes may also play a major role, the consequences and the conclusions that are reached here maintain a first-order validity.

The cornerstone: inclusions in enclaves and xenoliths

The use of MI for a better understanding of crustal melting has built primarily from the study of crustal enclaves hosted in the felsic peraluminous lavas of the Neogene Volcanic Province of SE Spain, and in particular from those hosted by the dacite of El Hoyazo, near Almería.

Figure 4. Andalusite with MI from a crustal xenolith in the Crd-bearing rhyolites of Lipari

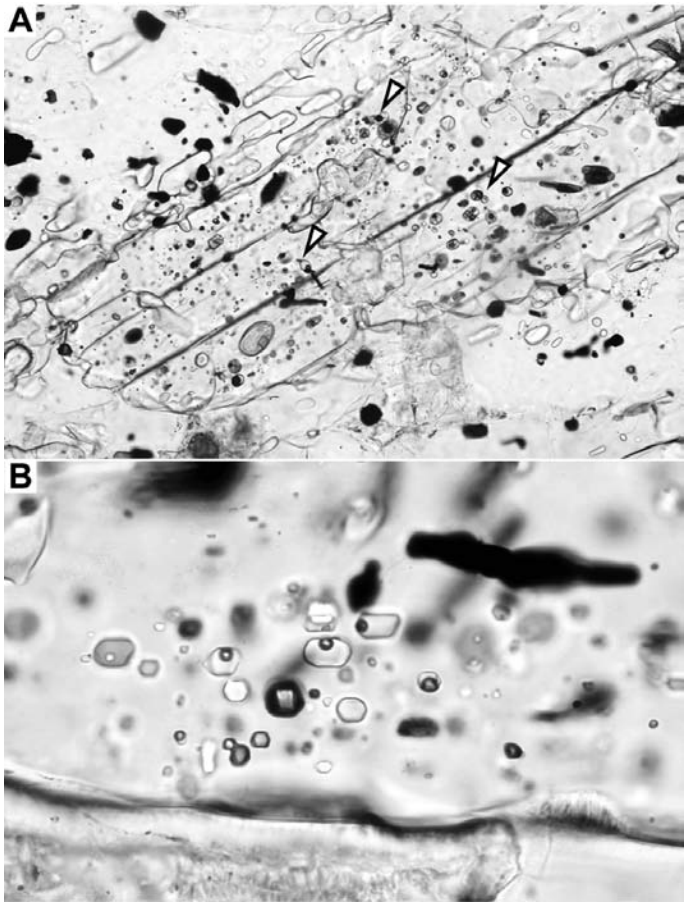

A: large scale view with arrows pointing at MI-rich zones. Width of view: 3.4 mm. B: close-up with detailed view of the glassy inclusions, each containing a shrinkage bubble. Width of view: 0.2 mm.

In this exceptional geological context, fragments of a partially melted crust situated at c. 20 km depth were rapidly brought to the Earth's surface by magma uprise, and quenched from temperatures of c. 800°C during submarine eruption of the host volcanic rocks. This allowed the

preservation of the mineralogical and textural features of an anatectic crystalline basement (Cesare *et al.*, 1997) similar to experimental charges but in hand sample sizes. Along with microstructures from the Spanish rocks, extensively described in the literature (Acosta Vigil *et al.*, 2010; Cesare, 2008 and references therein), here we also present new data from much smaller and less abundant crustal enclaves present in cordierite-bearing rhyolitic lavas from Lipari (S Italy, Barker, 1987), which display comparable features to those from SE Spain.

In the rocks from El Hoyazo, MI have been studied most extensively within garnet and plagioclase (e.g., Acosta Vigil *et al.*, 2007, 2010), but they are also hosted by biotite, cordierite, hercynitic spinel, K-feldspar, quartz, ilmenite, zircon, monazite, apatite and corundum (Cesare, 2008).

In the lower-pressure enclaves from Mazarrón (SE Spain) and from Lipari MI are also hosted in andalusite (Figure 4), and such occurrence has provided important constraints for the P-T location of the Al_2SiO_5 triple point (Cesare *et al.*, 2003a) as well as evidence that andalusite can coexist with a granitic melt (Clarke *et al.*, 2005). The arrangement of MI in minerals from the studied samples is commonly indicative of a primary trapping: zonal arrangement dominates in garnet and spinel (Figure 5A), where inclusions are commonly located in the core of crystals. In zircon, inclusions are distributed in a very thin annulus separating a detrital core from the syn-anatectic overgrowth (Cesare *et al.*, 2003b, 2009). In other hosts, especially plagioclase, MI occur throughout the mineral (Figure 5B, C) and may be so abundant to impart to the crystal a cloudy appearance. The occurrence of secondary MI, clearly associated with fractures postdating the host growth, is very rare (Cesare *et al.*, 2007).

Figure 5. Microstructures of MI in Spanish enclaves

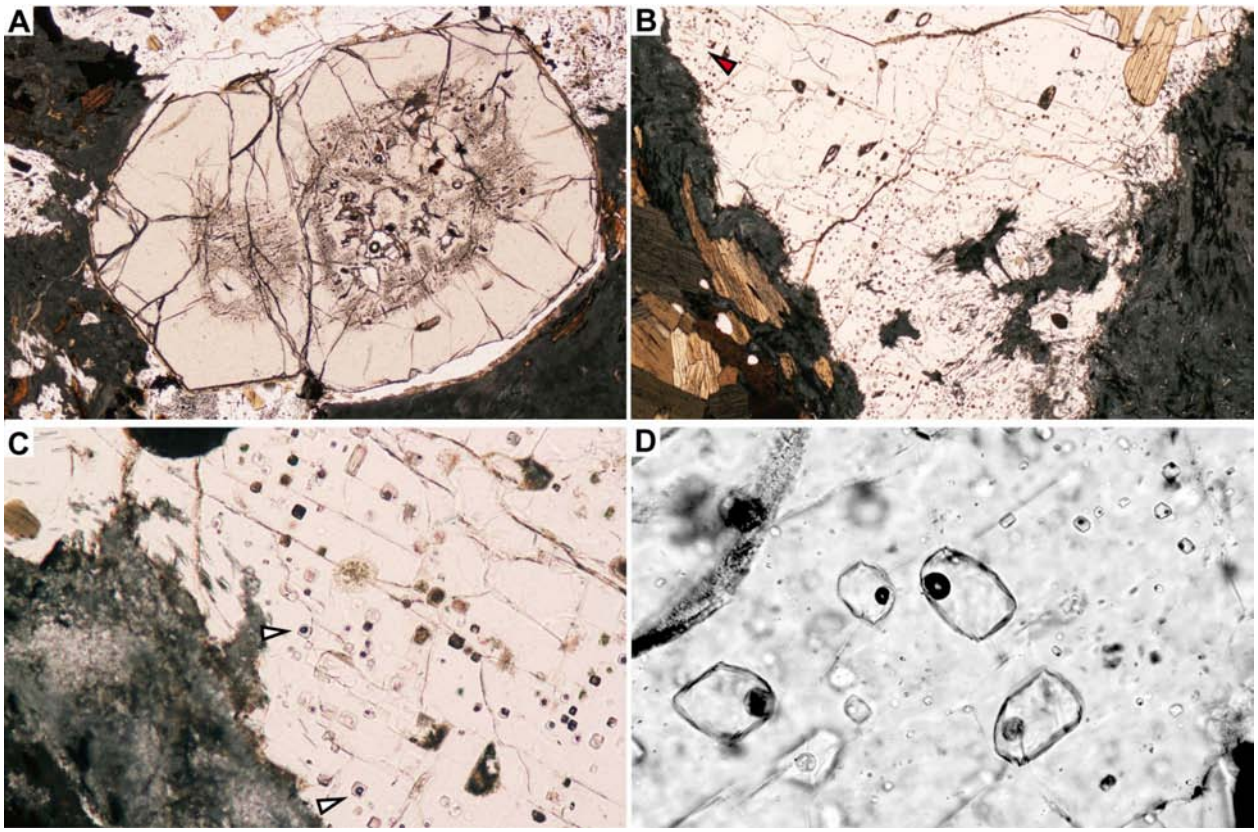

A: Zonal arrangement of MI in garnet from a residual enclave in the dacitic lavas of El Hoyazo, Spain. B: plagioclase containing MI throughout the crystal (El Hoyazo, Spain). Arrow indicates the area at the margin of plagioclase enlarged in (C). C: close-up of (B), showing that MI (negative crystals with shrinkage bubbles, arrows) are abundant also at the border of plagioclase. D: Large MI, with colorless, fresh glass and a shrinkage bubble, in plagioclase from an enclave (Mazarron, Spain). Widths of view: 8.4, 3.4, 0.85 and 0.35mm, respectively.

Figure 6. SEM microstructures of MI in spanish xenoliths

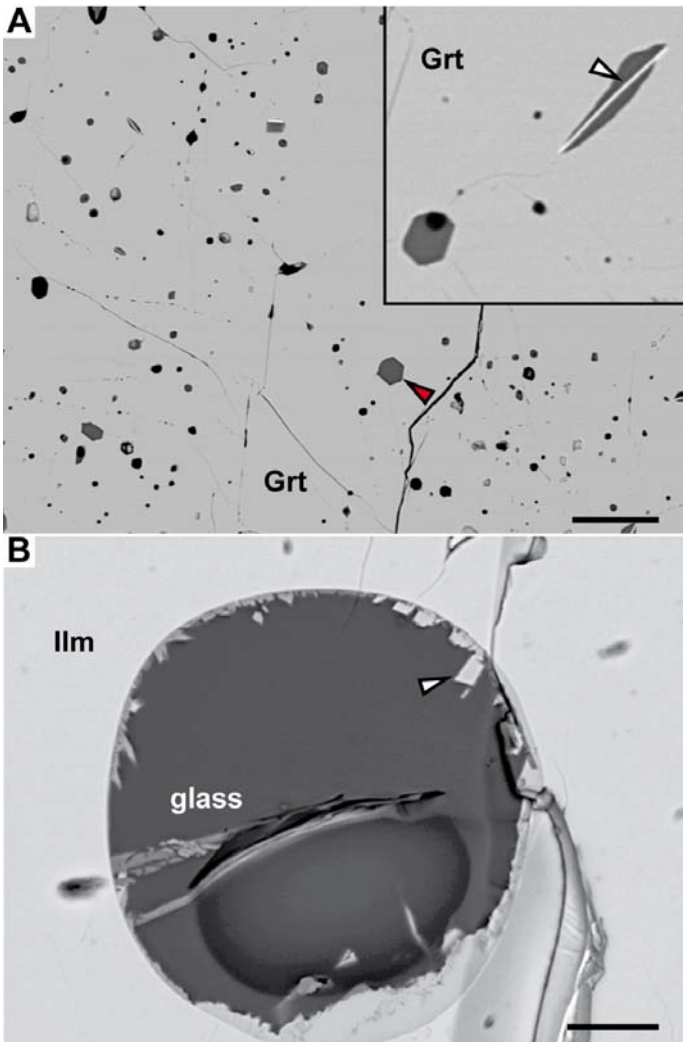

A: MI in garnet from an enclave of El Hoyazo. In the close-up of top-right two MI are enlarged: one with a well developed negative crystal shape, the other with an ilmenite needle (arrow) that is probably a trapped mineral. Scalebar: 50 µm. B: a large MI hosted in ilmenite in an enclave from El Hoyazo. The inclusion walls are coated by ilmenite daughter crystallites (arrow). Scalebar: 20 µm

The average size of MI is <30 µm, but exceptionally large inclusions may reach up to ˜100 µm in ilmenite, cordierite or plagioclase (Figures 5D and 6B). The shape is rarely irregular, more often rounded (zircon, ilmenite, cordierite) to negative crystal (garnet, spinel, plagioclase), or tubular (apatite), depending on the crystallographic control of the host mineral. The abundance of negative crystal shapes (Figure 6A) and the occurrence of "necking-down" phenomena (Acosta-Vigil *et al.*, 2007) indicates that solution/precipitation processes were efficient in modifying the shape of inclusions in order to diminish the surface free energy (Roedder, 1984).

The inclusions very often contain fresh, colorless, isotropic and undevitrified glass, and a single shrinkage bubble (Figures 4-6) that may be empty or contain fluids exsolved from the melt (mostly H_2O, Cesare *et al.*, 2007). Owing to the very fast cooling during submarine eruption, crystallization of “daughter minerals” from the glass is very rare and limited to some overgrowths or crystallites of ilmenite in MI in ilmenite (Figure 6B), or of alkali feldspar in MI in plagioclase (Acosta-Vigil *et al.*, 2007). While daughter minerals are rare, solid inclusions (or "trapped minerals", i.e., minerals that were already present during the formation of MI) may be widespread: the most common solid inclusion is graphite, particularly abundant in MI in plagioclase from the enclaves of El Hoyazo (Cesare and Maineri, 1999). Ilmenite (Figure 6A) and biotite are also observed as trapped minerals within MI in garnet. An origin as solid inclusions is attested by: (i) these minerals being partly enclosed in the host plagioclase or garnet; (ii) the fact that they occur only in part of the entire population of MI and in a non-systematic manner; (iii) the variable mineral/MI volume ratios; and (iv) the presence of these minerals also as single inclusions in the hosts. These observations support the hypothesis that, as frequently observed in previous studies of fluid and silicate melt inclusions, graphite, ilmenite or biotite lamellae acted as an imperfection at the growing crystal faces of the host mineral, and favoured the entrapment of MI.

The MI in enclaves and xenocrysts from felsic lavas described here are interpreted as primary, and therefore as indicating the coexistence of the host minerals with melt at the time of entrapment. These conditions were attained during partial melting of the metasedimentary protoliths, and hence the MI are interpreted as tiny droplets of the crustal anatectic melts as they were being produced.

Could the MI have formed by processes other than this, such as melting of solid inclusions already trapped within the host (Vernon, 2007)? If so, they would not indicate the growth of the host in the presence of melt, as melting could have occurred later in a geologically, and chronologically, separate event. The possibility that melting of solid inclusions (or “inclusion melting”) may produce MI with seeming primary origin has been discussed

by Cesare (2008) with special reference to the MI hosted in garnet at El Hoyazo.

Figure 7. Two examples of nanogranite inclusions

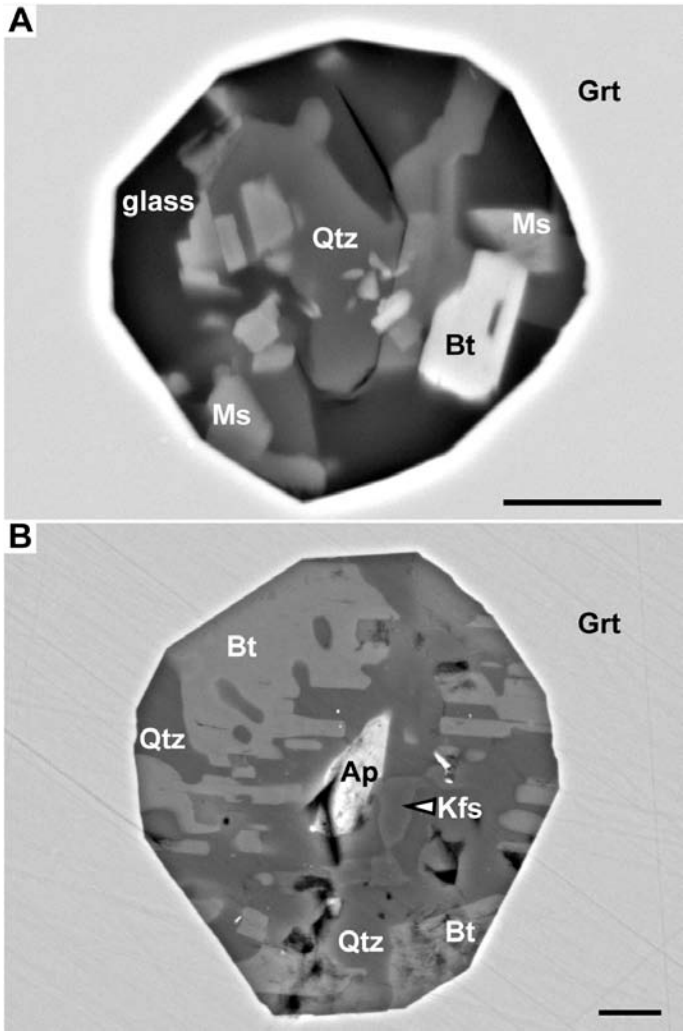

Two examples of *nanogranite* inclusion, hosted in garnet from the migmatites of Ronda (A) and the khondalites of the Kerala Khondalite Belt (B). Scalebars: 2 µm

It was shown that this process would be plausible only if all melt inclusions had been produced by the melting of an aggregate of solids and H_2O, each of them with exactly the same proportions of reactant phases as to melt completely. Here we reiterate the conclusion that this is "…geologically unresonable…" (Cesare, 2008), but specify – based on our recent experience on inclusion re-melting – that this process could work only if the inclusion trapped by the host was a *nanogranite* (see below). Nevertheless, the MI would have also originally contained a melt phase.

Owing to the combination of lack of crystallization and freshness of glass, these MI allow the geochemical characterization of natural crustal anatectic melts unaffected by retrograde or post-formation phenomena. Due to the exceptionally rare nature of these rocks, however, a thorough study of this genre could be undertaken for the first time only in the last decade (see below and Acosta-Vigil *et al.*, 2010, and references therein).

The development: *nanogranites* in migmatites

If anatectic melt is preserved as, and found in MI from unusual settings such as crustal enclaves in peraluminous felsic lavas, why have MI not been found in the more representative and common rocks that are produced by anatexis, i.e., migmatites and granulites? This question prompted the recent efforts of the writers, who started to (re)investigate rock samples from migmatite terrains worldwide looking for MI in peritectic minerals, in particular within garnet, thought to be one of the most promising hosts as it is formed by the incongruent melting of biotite. Of course, given the slow cooling (some millions of years compared with some minutes or days) that regionally metamorphosed and partially melted rocks have undergone, one should not expect to find glass anymore within MI, but rather a polyphase cryptocrystalline aggregate resulting from melt crystallization, as commonly observed in plutonic rocks (Bodnar and Student, 2006). This search led to the discovery (Cesare *et al.*, 2009) of "*nanogranites*" in garnets from the melanosomes of migmatitic granulites in the Kerala Khondalite Belt (KKB, India).

These are inclusions containing a granitic assemblage (quartz, feldspars and micas) made of crystals with micrometric or sub-micrometric grain-size (Figure 7). Despite the small size, the polycrystalline nature of these inclusions can easily be detected with a (good) optical microscope. For the sake of completeness, it should be noted that the inclusions in garnet previously described by Hartel *et al.* (1990) seem to be very similar to nanogranites, but this early report was not followed by detailed study. After the recent occurrence in the KKB, nanogranite inclusions have been also found in garnet from migmatites at Ronda (Spain), the Ivrea Zone and Ulten Zone (Italy) and the Himalayas (Nepal), and in ilmenite from Ronda. We also believe that the inclusions reported by

Henriquez & Darling (2009) in the Adirondacks (USA) should be nanogranites.

Figure 8. Typical fine-grained garnet crystal in migmatites from Ronda, showing MI-rich cores

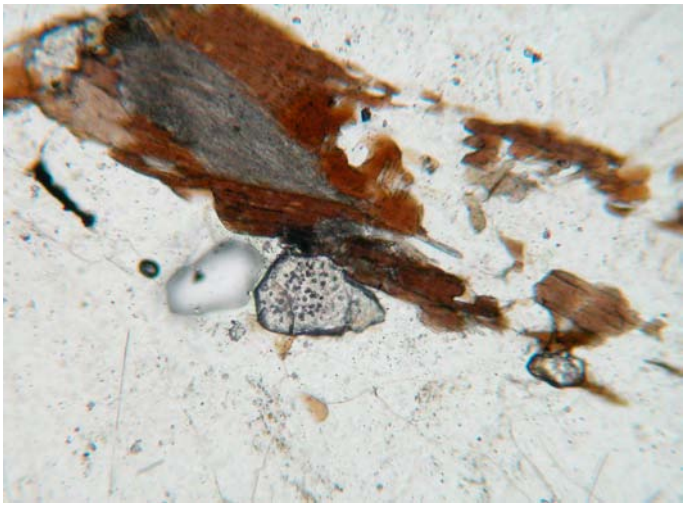

(see also Fig. 1A). Width of view: 0.6 mm.

Figure 9. Small MI (both nanogranite and glassy) hosted in garnet from a migmatite at Ronda

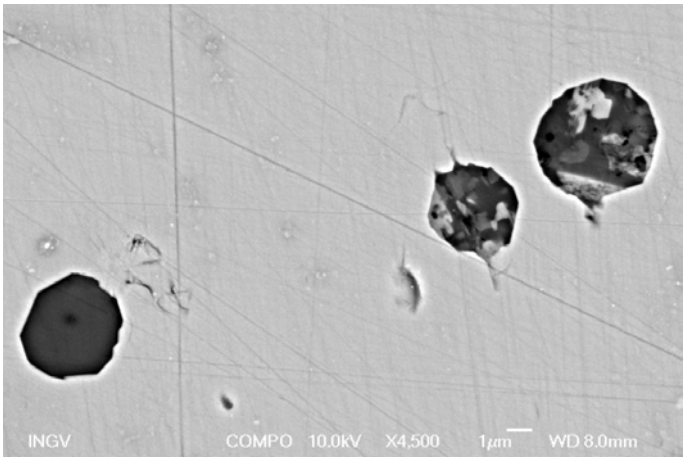

Although inclusions of nanogranite are rare in samples from the KKB and constitute scattered small clusters within the large garnet porphyroblasts, in most other occurrences they are arranged zonally in the cores of crystals (e.g., Figure 1A, B). An excellent example is provided by the migmatites of Ronda, where, regardless of the small crystal size (<0.2 mm), all the garnet cores are clouded with inclusions (Figures 1A and 8). Nanogranite inclusions are smaller than MI in the Spanish enclaves: the statistics on 244 measurements of nanogranites in the garnets from the KKB provided a mean and maximum diameter of 13 and 25 μm, respectively (Cesare *et al.*, 2009). In the garnets of Ronda inclusions are even smaller, often around 5 μm in diameter (Figure 9). Nanogranite inclusions in garnet are typically facetted, with a dodecahedral (Figure 10) negative crystal shape; more rarely they are round or tubular.

Figure 10. Examples of negative crystals in MI in garnet from the KKB (A) and the Ivrea Zone (B)

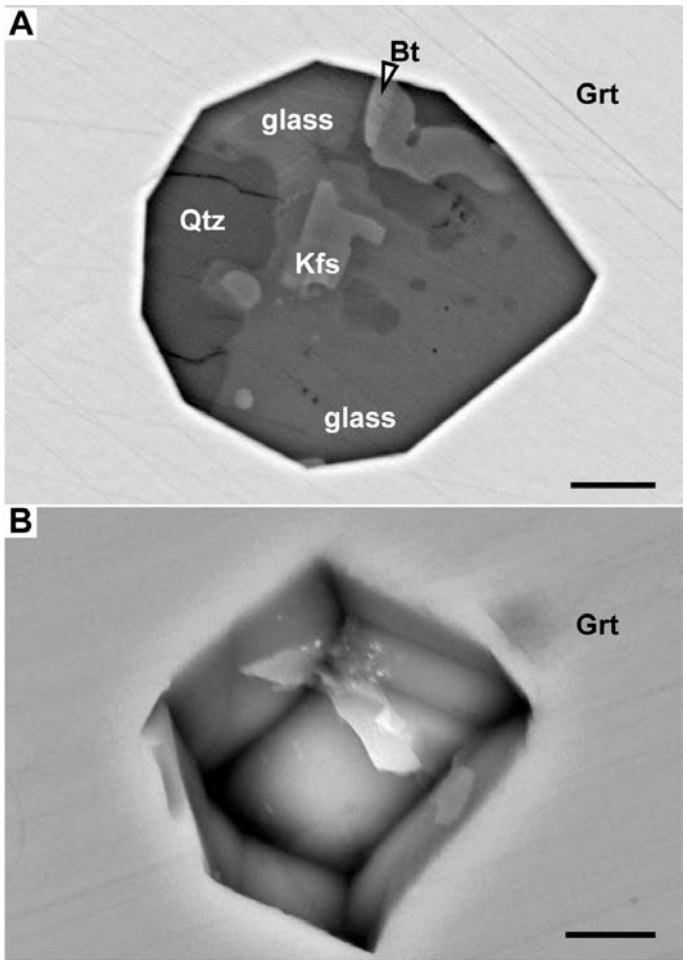

In the latter image, the MI has been emptied by mechanical removal during sample preparation, leaving a facetted rhombododecahedral pit in the garnet. Scale-bars: 2 μm

Inclusions contain aggregates of crystals with equigranular, hypidiomorphic to allotriomorphic texture. Sometimes granophyric to nano- to microgranophyric intergrowths of quartz and feldspars are also present (Figure 11A). Crystal grain-size ranges from hundreds of nm to a few μm, and minerals – especially micas - often appear to have grown from the inclusion walls, which represent preferred nucleation sites. Owing to these microstructural

and compositional features (see below), the cryptocrystalline aggregate found within inclusions was named "nanogranite" (Cesare *et al.*, 2009). SEM investigation of polished nanogranite inclusions exposed at the surface of host garnet suggests highly variable phase abundances and ratios. For example Figure 7b, showing a high proportion of biotite, would suggest that the trapped melt that crystallized wasn't an anatectic leucogranite, or that some peritectic biotite was entrained together with the melt in the inclusion. Since we were able to remelt completely the nanogranite inclusions (see below), since the composition of remelted glasses is homogeneous, and since the only unmelted crystals preserved in inclusions are zircon, apatite and ilmenite, we conclude that, owing to cut effects, the modal information that can be gained from SEM images are apparent and can be misleading, and that two-dimensional modal analysis of these small inclusions is unreliable. Other minerals, such as apatite, graphite, ilmenite, rutile and zircon, are also present in the nanogranites (e.g., Figures 11A to C); in most cases, these phases are interpreted as solid inclusions that were present at the mineral-melt interface during MI entrapment. This is particularly evident for the case of rutile needles associated with nanogranites in the garnets of Ronda (Figure 11B).

Figure 11. SEM microstructures of MI in migmatites

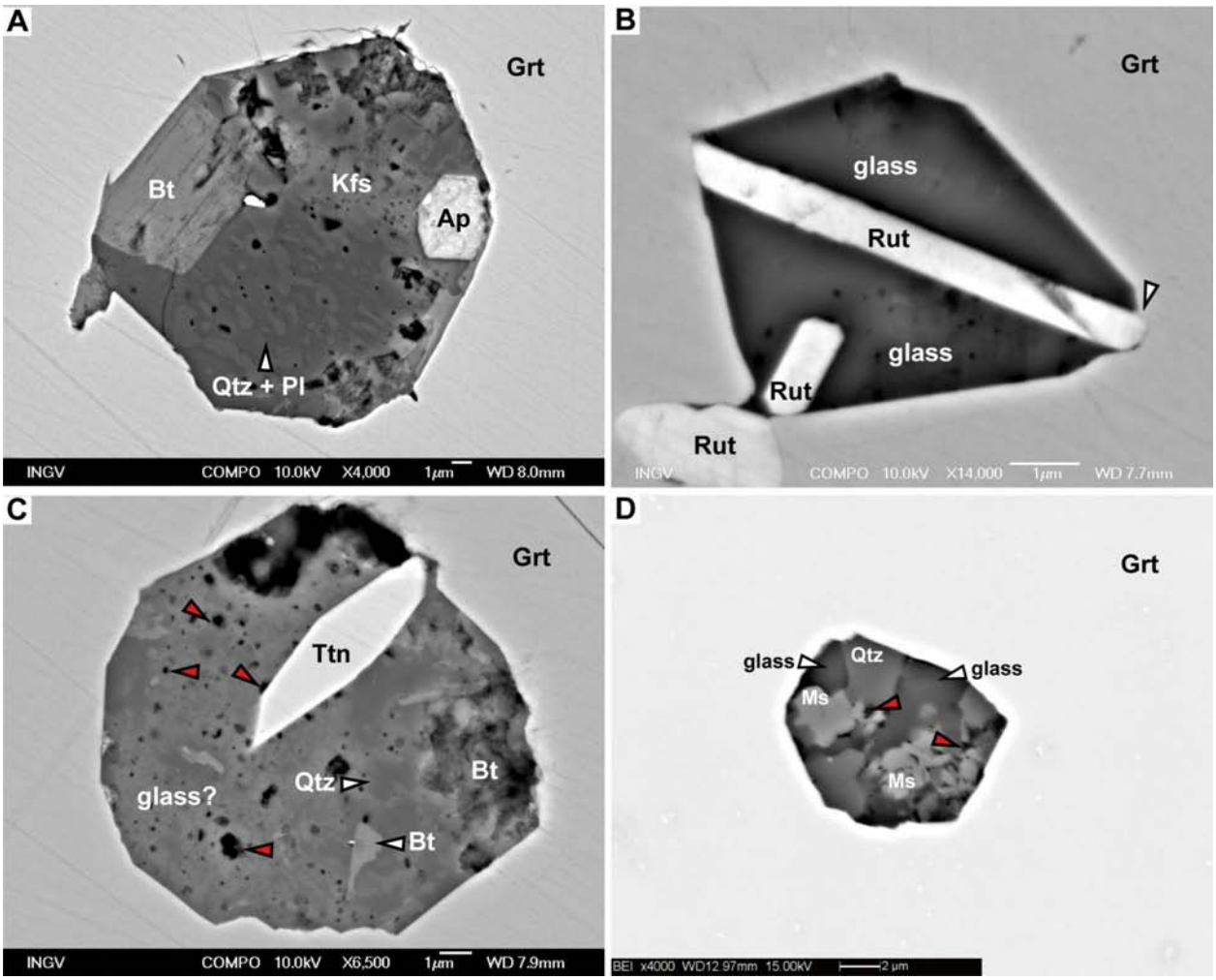

A: micrographic texture of finely intergrown quartz and plagioclase (arrow) in a nanogranite inclusion from the KKB. B: in some migmatites from Ronda rutile is the most common trapped mineral in the MI. The bottom right termination of the larger rutile needle (arrow) is partially enclosed in the host garnet, supporting the inference that rutile was trapped together with a melt droplet by the growing host. C, D: micro-to nano-porosity (red arrows) is often visible in nanogranites in samples from both KKB (C) and Ronda (D).

Nanogranite inclusions display a variable micro- to nano-porosity (Figures 11 C and D), that is commonly greater in the samples from Ronda. Although microcavities in inclusions exposed on the sample surface prepared for EMP or SEM investigation might be an artifact due to polishing, we have verified by Raman spectroscopy the presence of fluid-filled pores in nanogranite inclusions below the sample surface. These observations support the inference made by Cesare *et al.* (2009) that porosity forms by melt crystallization due to the higher density of solids with respect to the trapped melt. In the case of hydrous melts, the porosity is likely to contain exsolved fluids, in particular H_2O.

Diametrically opposite decrepitation tails often occur where the host shows evidence of deformation and microcracking (Figure 12). These inclusions and samples should be avoided as decrepitation may have induced or facilitated alteration of the original microstructural and compositional features of the inclusion.

Figure 12. Diametrically opposite decrepitation tails in MI in garnet

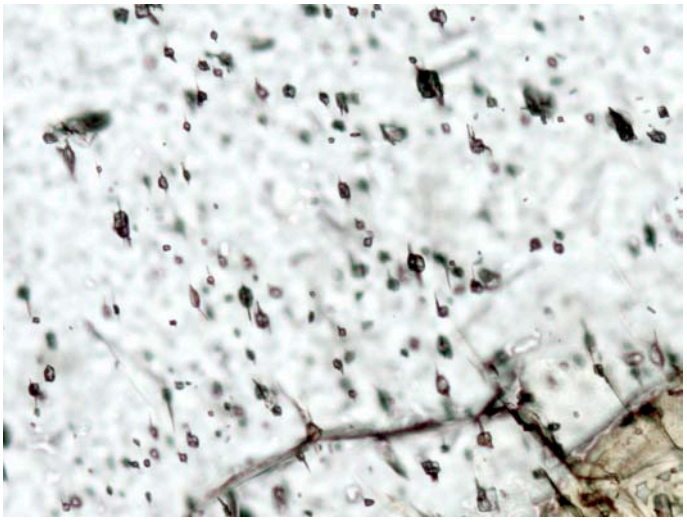

The orientation of microcracks is parallel to the major set of cracks in the host garnet. Width of view: 0.3 mm.

Microstructural features of the nanogranites that indicate crystallization from a melt are: (i) euhedral mineral shapes, in particular of biotite; (ii) high interfacial energy boundaries between minerals; (iii) nanogranophyric intergrowths, commonly recognized in plutonic rocks; and (iv) cuspate, thin elongate pockets or films of an unknow phase (possibly amorphous, still requires TEM investigation) that strongly resemble *melt pseudomorphs*, although 2-3 orders of magnitude thinner (Figure 13) than those previously described (Holness and Sawyer, 2008).

Nevertheless, the most convincing evidence that these inclusions represent trapped anatectic melts is that the melt phase, quenched as glass, can still be found within them (see below).

Figure 13. SEM microstructures of MI in migmatites

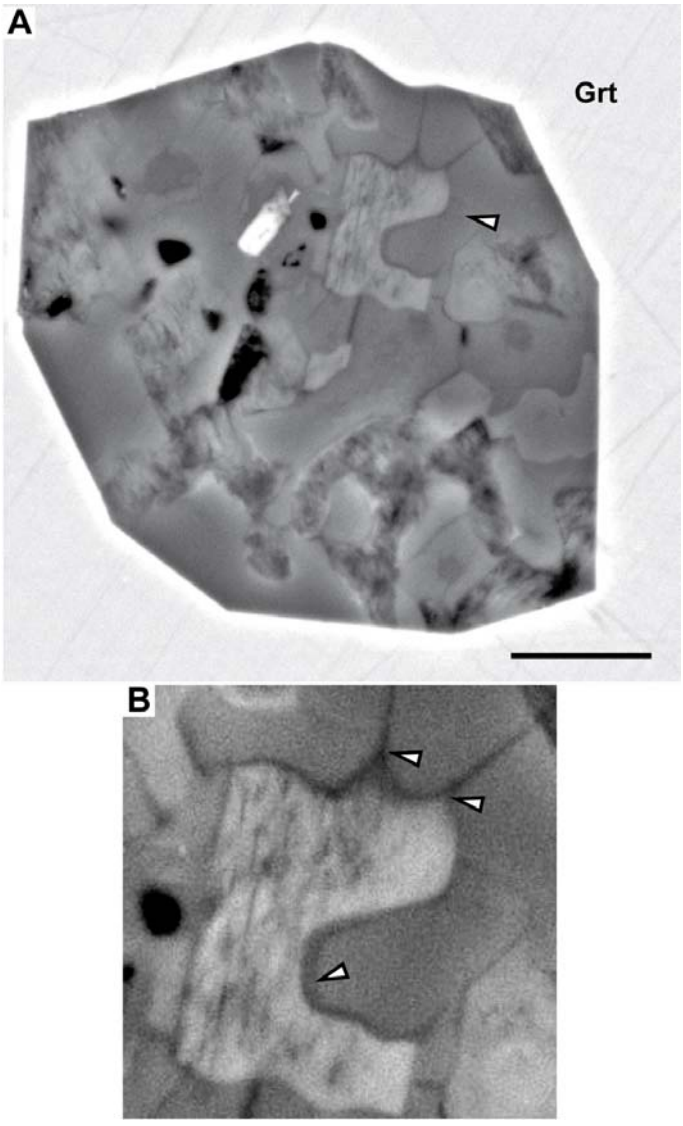

A) a nanogranite inclusion in garnet from the KKB. Arrow points to area enlarged in B. Scalebar: 2 µm. B) cuspate-lobate thin layers (arrows) of an undetermined phase define a microstructure that resemble *melt pseudomorphs* (reprinted from Cesare *et al.*, 2009).

The oddity: glass preservation in slowly cooled rocks

Cesare *et al.* (2009) showed that glass is preserved in some of the inclusions found in the garnets from the KKB granulites, in the same clusters containing the nanogranites and interspersed with them. The presence of silicic melt inclusions had also been reported in zircons from the migmatites of the Ulten Zone, Italy (Braga and Massonne, 2008). After these first studies, glass has also been found in inclusions within the garnets from the Ronda migmatites (Figure 14A). The amorphous nature of this phase has been proven by Raman spectroscopy, although the optical isotropy, SEM-homogeneous appearance and rhyolitic composition (see below) of this phase would suffice to demonstrate that it is a glass.

Figure 14. SEM microstructures of MI and remelted nanogranites

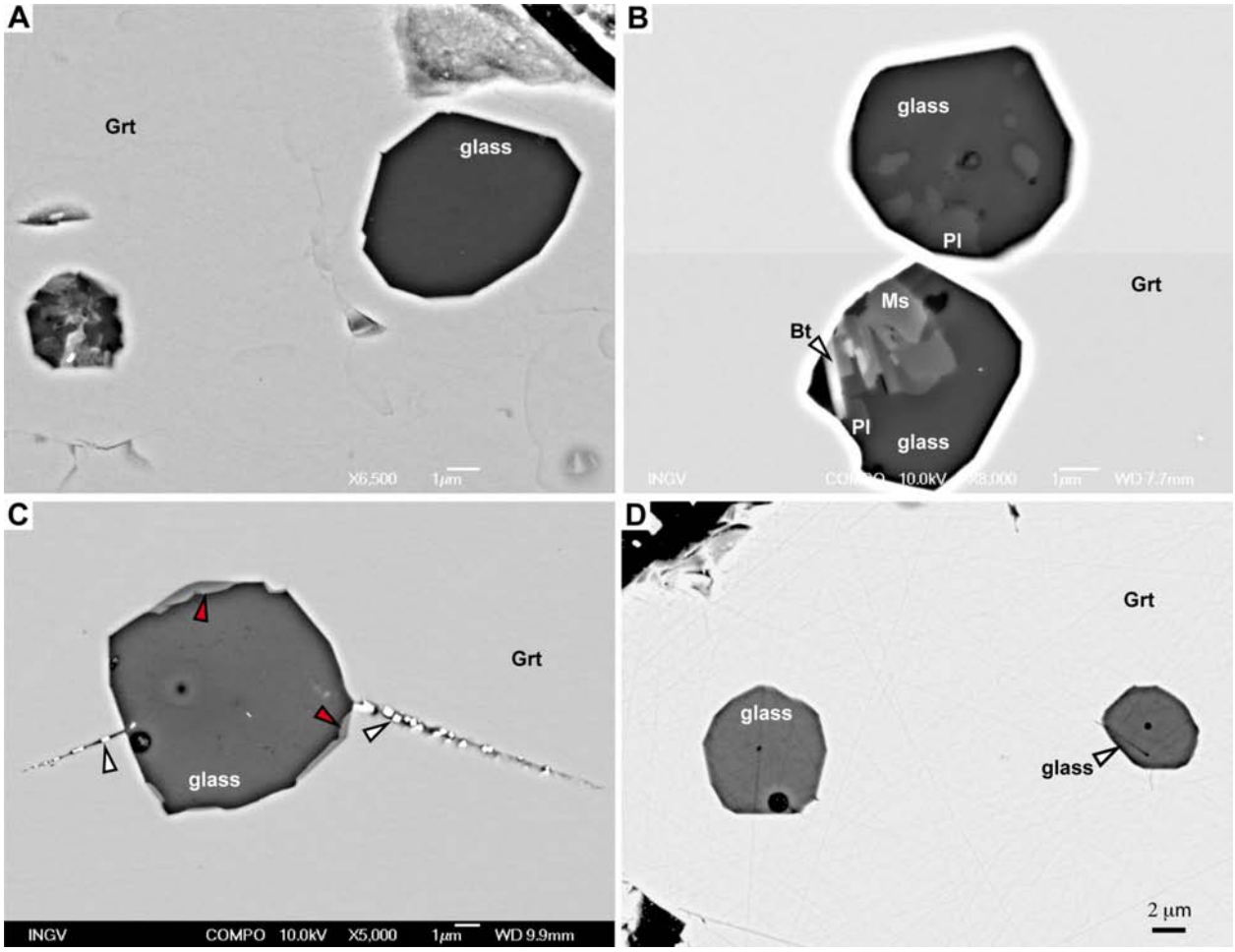

A: glassy inclusion (right), apparently larger than coexisting nanogranite (left) in the same cluster, hosted by garnet in a migmatite from Ronda. B: partially crystallized melt inclusions in garnet from Ronda. C: the product of remelting with an ambient-pressure heating stage of a nanogranite inclusion from the KKB rocks: decrepitation and some interaction with the host are visible (white arrows), along with thin overgrowths of peritectic mineral on inclusion walls (red arrows). D: the product of remelting in a piston cylinder of nanogranite inclusion from the Ronda migmatites: no decrepitation or incongruent melting of garnet walls is observed.

Recent work on the Ronda migmatites indicates that along with totally crystalline or completely glassy MI, partially crystallized inclusions are also common (Figure 14B): these contain variable proportions of glass, and the crystallized phases are generally quartz, biotite, muscovite and, more rarely, Na-rich plagioclase. Plagioclase is absent also in the few observed partially crystallized inclusions from the KKB.

While glassy inclusions are expected in phenocrysts from extrusive rocks, their xenoliths and enclaves, or pyrometamorphic rocks, all of which undergo sudden cooling from suprasolidus temperatures, the preservation of glass (quenched anatectic melt) in regionally metamorphosed and slowly cooled migmatites and granulites is a geological oddity. For example, even though migmatisation of metapelites around the Ronda peridotite could be modelled or considered in terms of a "regional contact metamorphism" that might have lasted only a few m.y., the available geochronological record (Cenki *et al.*, 2004) indicates that the KKB granulites took >60 m.y. to cool to <350°C from the peak UHT conditions. These timescales are generally considered incompatible with the solidification of melt to glass.

Moreover, considering that the presence of temperature gradients across the mineral hosts can be ruled out due to their small volume (a few mm^3), the above problem has two (possibly connected) aspects: (i) the presence of glass, and (ii) the coexistence, a few µm apart, of glassy and (partially) crystallized inclusions. This translates into two questions: (1) what is the cause of the lack of melt crystallization? (2) Why did crystallization occur only in some inclusions?

Concerning the second question, there may be several possible answers, such as: i) differences in composition among melts in different inclusions, or ii) heterogeneous distribution of nucleation sites among inclusions (e.g., irregularities on inclusion walls' surface, trapped minerals, etc.), or iii) heterogeneous microfracturing/decrepitation that promoted nucleation, or iv) difference in inclusion size, with inhibition of nucleation in the smaller ones. Measurements of the diameters of MI in garnets from the KKB rocks led Cesare *et al.* (2009) to the preferred explanation that inclusion size was the main parameter affecting the behaviour on crystallization, and that, as already shown in acqueous solutions (Putnis *et al.*, 1995), crystallization was inhibited in the smaller inclusions (see also Holness and Sawyer, 2008).

The pore size effect, supported by the KKB samples, seems to find less evidence in the MI from Ronda, where glassy inclusions appear to have the same range of size (Figure 9) or even be smaller than fully crystallized inclusions (Figure 14A). Based on the currently available data we can suggest that ˜5-10 µm may represent a threshold diameter under which crystallization is inhibited, and that in each inclusion additional factors, such as surface irregularities or preexisting nuclei, may play an additional role.

More data and case studies are required to obtain a definitive solution to the paradox of glass preservation, but regardless of such uncertainty, and albeit rare, the glassy MI constitute an extremely important feature: since their composition is comparable with that of crystallized nanogranites (see below), glassy MI are the most primary examples of anatectic melts that can be found in migmatites and granulites, and their composition can be analyzed – within the analytical limitations imposed by their small size – without having to manipulate the inclusion, e.g. by re-melting the nanogranite.

The challenge: analysis of tiny inclusions

The glassy, partially crystallized or nanogranite inclusions from the case studies analysed so far are small, especially at Ronda, where their diameters are often <5µm. The small size represents an analytical challenge as it is near or below the limits of the spatial resolution of several conventional microanalytical techniques. It should be pointed out that the primary difficulty for the analysis is sample preparation, as uncovering and polishing the inclusions for SEM and EMP characterization is very difficult and often results in the mechanical removal of the inclusion content.

Concerning the major element analysis of crystals, the electron microprobe often provides compositions that are contaminated by adjacent or underlying phases. This problem could be solved by using the new generation of FEG-based microprobes, as well as standardized EDS analysis by SEM. An additional and important problem is the loss of Na from the inclusion material, that increases by focussing the beam size and increasing the beam current. Sodium loss is particularly important during the analysis of hydrous felsic glasses (Morgan and London, 1996, 2005). In the absence of a N_2-cooled EMP cryostage (e.g. Clemens, 2009), our approach for the analysis of silicate glass in inclusions has been that suggested by Morgan and London (1996, 2005): to correct the data for Na loss by comparison with the behaviour, at the same analytical conditions, of rhyolitic glass standards with variable H_2O contents (e.g. Cesare *et al.*, 2009).

It is the bulk composition of the melt that produced the nanogranite that is of major petrological and geochemical interest, rather than the composition of the individual mineral phases that constitute the nanogranite.

Therefore, nanogranites and partially crystallized inclusions are re-melted, and the glass obtained upon rapid quenching is analysed with the techniques described above. Remelting has been performed at ambient pressure using the high-temperature stage, a routine technique in igneous petrology (Frezzotti, 2001); although in general the composition of the remelted nanogranite is comparable with that of preserved glassy inclusions found in the same crystal (see below, and Cesare *et al.*, 2009), the results are not entirely satisfactory as remelting by the high-temperature stage often induces decrepitation accompanied by volatile loss and interaction with host mineral (Figure 14C). As a consequence nanogranites have been also remelted in a piston cylinder. Experiments at 5 kbar with the samples from Ronda have produced the complete remelting of crystalline inclusions, without decrepitation or production of peritectic phases (Figure 14D). This technique, although time-consuming, appears to be more suitable than the heating stage for restoring the bulk composition of the primary melt in the inclusion. In this regard, perfect remelting without the growth of peritectic phases or the retention of mineral residues supports the idea expressed above that the melting of preexisting solid inclusions suggested by Vernon (2007) may be realistic, but requires: 1) the presence of nanogranite as inclusions - i.e. the rock must have already undergone a previous partial melting event with growth of peritectic phases and MI entrapment; and, 2) the onset, in the new anatectic event, of the same PT conditions as those which led to the nanogranite formation, to obtain a perfect remelting of the inclusion.

If the MI really behave as closed systems, remelting without MI decrepitation potentially allows any exsolved fluid to be re-dissolved into the melt phase, and the primary fluid content of the anatectic melt to be measured after quenching. A first-order approximate indication of the melt volatile content can be obtained by the difference between 100 and the EMP total, if the analytical set-up follows the recommendations of Morgan and London (1996, 2005). Because H_2O is the main volatile in S-type felsic magmas, a more precise quantification of the volatile concentrations in glassy or remelted inclusions can be performed by SIMS, IR- or Raman spectroscopy; given the small size of the MI, the most promising method among these appears to be Raman spectroscopy (Thomas *et al.*, 2006).

The results: composition of anatectic melts

The chemical aspects of our research on MI are beyond the scope of this paper. Details concerning the chemistry of anatectic melts in the enclaves from El Hoyazo can be found in Acosta-Vigil *et al.* (2007, 2010) and in the literature quoted therein, whereas the chemical analysis of MI in migmatites and granulites is still work in progress. Here we provide only a few insights for the potential of this research.

Figure 15. CIPW quartz-albite-orthoclase normative compositions (in wt%) of glasses from El Hoyazo enclaves and KKB and Ronda migmatites

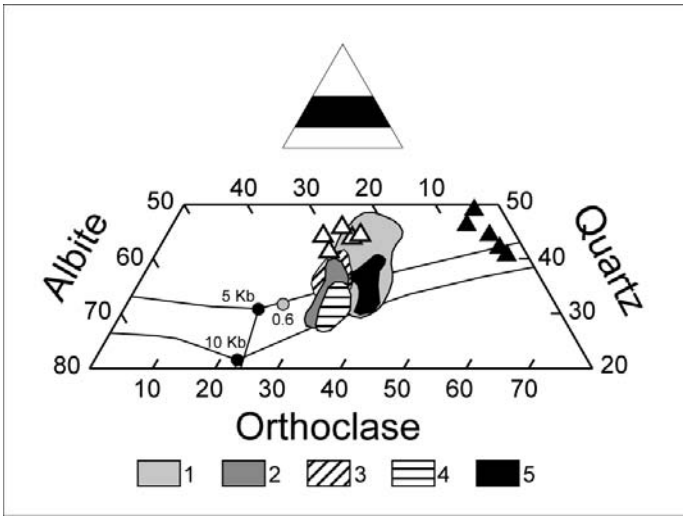

Glasses from El Hoyazo: 1: MI in plagioclase; 2: MI in garnet; 3: MI in Crd; 4: MI in Ilm; 5: matrix glasses. Melt inclusions from the KKB migmatites: filled triangles. Melt inclusions from the Ronda migmatites: white triangles. Black dots and lines in the quartz-albite-orthoclase diagram refer to eutectic points and cotectic lines, respectively, of the H_2O-saturated haplogranite system at 5 and 10 kbar. Gray dot refers to the eutectics point of the H_2O-undersaturated haplogranite system at a_{H2O}=0.6.

The major element chemical compositions and some trace element concentrations of the MI analyzed so far are summarized in Table 1 (see Appendix A) and Figure 15. Inclusions from both enclaves and migmatites have a peraluminous, granitic composition, in agreement with results from the experimental anatexis of Al-rich metasedimentary parent rocks (Le Breton and Thompson, 1988; Vielzeuf and Holloway, 1988; Patiño Douce and Johnston, 1991). It is important to note that in each of the investigated cases of migmatites/granulites, the KKB and Ronda, the compositions of remelted nanogranites and

coexisting glassy inclusions overlap within analytical uncertainty.

Considering the analyses of all inclusions, they show systematic compositional patterns and variations. At El Hoyazo the MI in the different host phases of the enclaves (cordierite, garnet, ilmenite and plagioclase) have slightly different compositions. The integration of textural and chemical information suggests that MI record the progressive entrapment of compositionally evolving melts formed during the prograde anatexis of these rocks. For instance, the composition of MI in plagioclase and garnet indicates relatively low (700-750 °C) temperatures of entrapment and therefore may supply information on the early anatectic history of the rock (Acosta-Vigil *et al.,* 2010).

Conversely, in the KKB granulites, the ultrapotassic and anhydrous compositions of MI in garnets are very far from a "minimum melt" and point to melting temperatures well above minimum or eutectic temperatures, in agreement with the ultra-high temperature (>900 °C) origin of the rock (Cesare *et al.*, 2009). Similar ultrapotassic rhyolites have been obtained by experimental melting of a pelitic protolith at P-T conditions of 5 kbar, 900 °C (e.g., Droop *et al.*, 2003).

Are the chemical compositions discussed above unaffected by post-entrapment processes? In other words, are they representative of primary anatectic melts? Post-entrapment phenomena are well known in MI studies in igneous rocks, and may range from subtle to major: on one side there might be diffusion among the host and the melt or its crystallization/solidification products; on the other decrepitation and opening of the system, with access of fluids through microcracks, may occur; and in-between there is host-melt interaction with dissolution or crystallization (stable or metastable) at inclusion walls. Concerning this latter phenomenon – growth of host within the inclusion – it is important to remind again the major difference in mode of entrapment existing between the MI in migmatites and granulites described here and those from igneous rocks, especially extrusive. As noted above most MI in migmatites are expected to form during melt production, entrapped by a peritectic mineral growing with the melt, whereas MI in igneous rocks form during cooling and are trapped by a host mineral that is crystallizing from the melt. Accordingly, the relationships between solid host and entrapped melt are radically different: inspection of stability phase relationships indicates that when the host is a peritectic mineral, it should not precipitate from the melt within the inclusion. The type and extent of post entrapment modifications can be assessed by careful microstructural observation combined with chemical mapping and analysis. In the glassy inclusions at El Hoyazo, modifications were virtually negligible and occurred by minor crystallization of daughter alkali feldspar at the walls of inclusions hosted in plagioclase (Acosta-Vigil *et al.*, 2007). In the MI in migmatites we expect Fe-Mg diffusion between the garnet host and biotite from the nanogranites. Moreover, more extensive reequilibration might occur during slow cooling if the melt was hydrous. Nonetheless, experimental remelting by the piston cylinder technique, by reproducing P-T conditions close to those of MI entrapment, should drive the melt back (close) to its primary composition.

An additional and important question is whether the composition of MI are representative of that of the bulk melt in the system at the time of MI entrapment. For the case of El Hoyazo, and based on a large number of major (˜300) and trace element (˜50) analyses, Acosta-Vigil *et al.* (2007, 2010) have shown that MI compositions do not represent exotic boundary layers or local compositions but may correspond to those of the bulk melt regarding major elements and incompatible trace elements. They also recognized, however, that the concentrations of the compatible trace elements were likely affected by local disequilibrium phenomena at the mineral-melt interface, and, therefore were not representative of the bulk melt. More information on this problem requires the acquisition of, and comparison among, large and high quality analytical datasets on many occurrences worldwide.

The outlook

Glassy inclusions in metasedimentary enclaves, as well as their crystallized counterpart - nanogranites - in migmatites and granulites, contain the melt phase that was being produced during incongruent crustal melting and that was enclosed by the peritectic minerals growing simultaneously. Trapped during a prograde event of magma formation, these MI differ from the granitic inclusions found in minerals from plutonic and volcanic rocks of granitoid composition (e.g., Yang & Bodnar, 1994; Thomas *et al.*, 2002; Anderson, 2003; Webster, 2006), which formed during magma crystallization upon cooling.

There is still a lot of work to be done in order to understand the best ways to observe and remelt nanogranites, to determine how representative are MI of the bulk melt composition in the system, and how and to which extent the retrograde history affects MI by interaction with the host. Nonetheless, our finding of MI in migmatites and granulites has two important consequences.

From a microstructural point of view, recognition of MI (in particular of nanogranites) is a proof that a rock was partially melted at some time in its history. While in many migmatites this can be inferred by several other methods (reviewed by Vernon, 2011) there are cases where MI may be *the only* textural evidence left of anatexis. One example are polymetamorphic basements, such as some internal crystalline massifs in the Alps - Gran Paradiso (Biino and Pognante, 1989) and Dora-Maira (Compagnoni & Rolfo, 2000) - where Variscan anatexis was followed by an Alpine evolution involving HP-LT metamorphism and subsequent greenschist-facies reequilibration. In this case, especially in the zones of intense deformation, it is not uncommon that textural and mineralogical evidence of anatexis has been totally erased, except for the persistence of garnet relicts that may contain nanogranite inclusions. Because of this, we believe that the occurrence of nanogranites should be included among the most reliable microstructural criteria for the former presence of felsic melt (e.g., Vernon, 2011).

From a chemical point of view, these nm- to µm-scale objects, so far studied in igneous rocks, allow for the direct analysis of natural anatectic melt compositions, overcoming the problems and uncertainties that are involved in assuming leucosomes as representative of anatectic melts in regional-scale migmatites (Brown, 2010). Melt inclusion compositions will thus provide much more reliable chemical constraints to the petrological and geochemical models of crustal melting processes. For example, trace element analyses of MI can open new developments for geochemistry and thermobarometry, as shown by Acosta-Vigil *et al.* (2010).

With the fast development of microanalytical tools, MI studies in migmatites and granulites may become a routine object of study in crustal petrology. At present, they also represent a promising subject for the successful application of cutting-edge techniques (for petrological purposes) such as nanoSIMS, ToF-SIMS (Rost *et al.*, 2009), FIB TEM and synchrotron-based µ-XRD, µ-XRF and µ-CT.

We believe that many occurrences of MI have been overlooked because they simply were not searched for, and that they will be uncovered by careful re-investigation of migmatite and granulite samples worldwide. The preservation of inclusions depends on the chemical and mechanical behavior of the host-inclusion system during the post-entrapment history of the rock. Since microfracturing would allow the infiltration of fluids and modification of the primary melt composition or nanogranite assemblage, MI should be targeted in the most chemically inert and mechanically strong mineral hosts (e.g., garnet, ilmenite, rutile, spinel, zircon) from the least deformed rock domains.

Acknowledgements

We thank the Journal of the Virtual Explorer editors for inviting this contribution, and Mike Brown and Linc Hollister for reviewing it. Financial support from Italian Ministry of Education, University and Research (grant PRIN 2007278a22 to BC), from a Ramón y Cajal research contract to AAV, and from Ministerio de Ciencia e Innovación of Spain (projects CTM2005-08071-C03-01, CSD2006-0041 and CGL2007-62992 to AAV).

References

Acosta-Vigil, A., Buick, I., Hermann, J., Cesare, B., Rubatto, D., London, D., Morgan VI, G., (2010). Mechanisms of crustal anatexis: a geochemical study of partially melted metapelitic enclaves and host dacite, SE Spain. Journal of Petrology 51: 785-821.

Acosta-Vigil, A., Cesare, B., London, D. & Morgan VI, G.B. (2007) Microstructures and composition of melt inclusions in a crustal anatectic environment, represented by metapelitic enclaves within El Hoyazo dacites, SE Spain. Chemical Geology 237, 450–465.

Anderson, A.T. (2003) An introduction to melt (glass ± crystals) inclusions. In Samson, I., Anderson, A., & Marshall, E., (Eds.): Fluid Inclusions: Analysis and Interpretation. Mineralogical Association of Canada, Vancouver, BC, Short Course Series 32: 353-364.

Barker, D.S. (1987) Rhyolites contaminated with metapelite and gabbro, Lipari, Aeolian Islands, Italy: products of lower crustal fusion or of assimilation plus fractional crystallization? Contributions to Mineralogy and Petrology 97: 470-492.

Biino, G. & Pognante, U. (1989) Palaeozoic continental-type gabbros in the Gran Paradiso nappe (Western Alps, Italy): Early-Alpine eclogitization and geochemistry. Lithos 24: 3-19.

Bodnar, R.,J. & Student, J.J. (2006) Melt inclusions in plutonic rocks: petrography and microthermometry. In: Webster, J.D. (ed.): Melt inclusions in plutonic rocks. Mineralogical Association of Canada, Short Course 36, 1-26.

Braga, R. & Massonne, H.J. (2008) Mineralogy of inclusions in zircon from high-pressure crustal rocks from the Ulten Zone, Italian Alps. Periodico di Mineralogia 77: 43-64.

Büsch, W., Schneider, G. & Mehnert, K.R. (1974) Initial melting at grain boundaries. Part II: melting in rocks of granitic, quartz dioritic, and tonalitic composition. Neues Jahrbuch für Mineralogie, Monatshefte 345-370.

Brown, M., 2010. The spatial and temporal patterning of the deep crust and implications for the process of melt extraction. Philosophical Transactions of the Royal Society A, 368, 11-51.

Cenki, B., Braun, I. & Bröcker, M. (2004) Evolution of the continental crust in the Kerala Khondalite Belt, southernmost India: Evidence from Nd isotope mapping combined with U-Pb and Rb-Sr geochronology. Precambrian Research 134: 275–292.

Cesare, B. (2008) Crustal melting: working with enclaves. In: Sawyer, E.W. & Brown, M. (eds.) Working with Migmatites. Mineralogical Association of Canada, Short Course 38: 37–55.

Cesare, B., Ferrero, S., Salvioli-Mariani, E., Pedron, D. & Cavallo, A. (2009). Nanogranite and glassy inclusions: the anatectic melt in migmatites and granulites. Geology 37: 627-630.

Cesare, B., Gomez-Pugnaire, M.T. & Rubatto, D. (2003b) Residence time of S-type anatectic magmas beneath the Neogene Volcanic Province of SE Spain: a zircon and monazite SHRIMP study. Contributions to Mineralogy and Petrology 146: 28–43.

Cesare, B. & Maineri, C. (1999) Fluid-present anatexis of metapelites at El Joyazo (SE Spain): constraints from raman spectroscopy of graphite. Contributions to Mineralogy and Petrology 135: 41-52.

Cesare, B., Maineri, C., Baron Toaldo, A., Pedron, D. & Acosta-Vigil, A. (2007) Immiscibility between carbonic fluids and granitic melts during crustal anatexis: a fluid and melt inclusion study in the enclaves of the Neogene Volcanic Province of SE Spain. Chemical Geology 237: 433–449.

Cesare, B., Marchesi, C., Hermann, J. & Gomez-Pugnaire, M.T. (2003a) Primary melt inclusions in andalusite from anatectic graphitic metapelites: Implications for the position of the Al2SiO5 triple point. Geology 31: 573-576.

Cesare, B., Rubatto, D. & Gómez-Pugnaire, M.T. (2009) Do extrusion ages reflect magma generation processes at depth? An example from SE Spain. Contributions to Mineralogy and Petrology 157: 267-279.

Cesare, B., Salvioli Mariani, E. & Venturelli, G. (1997) Crustal anatexis and melt extraction during deformation in the restitic xenoliths at El Joyazo (SE Spain). Mineralogical Magazine 61, 15–27.

Clarke, D.B., Dorais, M., Barbarin, B., Barker, D., Cesare, B., Clarke, G., el Baghdadi, M., Erdmann, S., Förster, H-J., Gaeta, M., Gottesmann, B., Jamieson, R.A., Kontak, D.J., Koller, F., Gomes, C.L., London, D., Morgan, VI G.B., Neves, L.J.P.F., Pattison, D.R.M., Pereira, A.J.S.C., Pichavant, M., Rapela, C., Renno, A.D., Richards, S., Roberts, M., Rottura, A., Saavedra, J., Sial, A.N., Toselli, A.J., Ugidos, J.M., Uher, P., Villaseca, C., Visonà, D., Whitney, D.L., Williamson, B. & Woodard, H.H. (2005) Occurrence and origin of andalusite in peraluminous felsic igneous rocks. Journal of Petrology 46:441–472.

Clemens, J.D. (2009) The message in the bottle: “Melt” inclusions in migmatitic garnets. Geology 37: 671-672.

Clocchiatti, R. (1975) Les inclusions vitreuses des cristaux de quartz. Étude optique, thermo-optique et chimique. Applications géologiques, Mémoires de la Société géologique de France 122: 1-96.

Compagnoni, R. & Rolfo, F. (2000) Characteristics of UHP pelites, gneisses, and other unusual rocks. In: Ernst, W.G. & Liou, J.G. (eds.): Ultra-high pressure metamorphism and geodynamics in collision-type orogenic belts. Geological Society of America, International Lithosphere Program 344: 74–92.

Droop, G.T.R., Clemens, J.D. & Dalrymple, J. (2003) Processes and conditions during contact anatexis, melt escape and restite formation: the Huntly Gabbro complex, NE Scotland. Journal of Petrology 44: 995-1029.

Fenn, P.M. (1977) The nucleation and growth of alkali feldsaprs from hydrous melt. Canadian Mineralogist 15: 135-161.

Frezzotti, M.L. (2001) Silicate melt inclusions in magmatic rocks: applications to petrology. Lithos 55: 273–299.

Goldstein, R.H. (2003) Petrographic analysis of fluid inclusions. . In Samson, I., Anderson, A., & Marshall, E., (Eds.): Fluid Inclusions: Analysis and Interpretation. Mineralogical Association of Canada, Vancouver, BC, Short Course Series 32: 9-53.

Hartel, T. H. D., Pattison D. R. M., Helmers, H. & Maaskant, P. (1990) Primary granitoid-composition inclusions in garnet from granulite facies metapelite: Direct evidence for the presence of a melt? Geological Association of Canada 15: 54 (abstract).

Henriquez, J.L. & Darling, R.S. (2009) Zircon clinging inferred anatectic melt inclusions from Adirondack garnet: Geological Society of America, Abstracts with Programs, 42-1: 161.

Hollister, L.S. & Crawford, M.L. (1981) Fluid Inclusions: Applications to Petrology. Mineralogical Association of Canada Short Course Handbook 6, 304 p.

Holness, M.B. (2010) Decoding dihedral angles in melt-bearing and solidified rocks. Journal of the Virtual Explorer, Electronic Edition, ISSN 1441-8142, volume 35, paper 2. In: Forster, M.A & FitzGerald J.D, (eds.), The Science of Microstructure - Part I, 2010.

Holness, M.B., Cesare, B. & Sawyer E.W. (2011) Melted rocks under the microscope: microstructures and their interpretation. Elements, in prep.

Holness, M.B. & Sawyer, E.W. (2008) On the pseudomorphing of melt-filled pores during the crystallization of migmatites. Journal of Petrology 49: 1343–1363.

Le Breton, N. & Thompson, A.B. (1988) Fluid-absent (dehydration) melting of biotite in metapelites in the early stages of crustal anatexis. Contributions to Mineralogy and Petrology 99: 226-237.

Means, W.D., (1989) Synkinematic microscopy of transparent polycrystals. Journal of Structural Geology 11: 163-174.

Means, W. D. & Park, Y. (1994). New experimental approach to 463–474. understanding igneous texture. Geology 23, 323–326.

Mehnert, K.R., Büsch, W. & Schneider, G. (1973) Initial melting at grain boundaries of quartz and feldspar in gneisses and granulties. Neues Jahrbuch für Mineralogie 4: 3563-3592.

Morgan, G.B., VI & London, D. (1996). Optimizing the electron microprobe analysis of hydrous alkali aluminosilicate glasses. American Mineralogist 81: 1176–1185.

Morgan, G.B., VI & London, D. (2005) Effect of current density on the electron microprobe analysis of alkali aluminosilicate glasses. American Mineralogist 90: 1131–1138.

Patiño Douce, A.E. & Johnston, A.D. (1991) Phase equilibria and melt productivity in the pelitic system: implications for the origin of peraluminous granitoids and aluminous granulites. Contributions to Mineralogy and Petrology 107: 202-218.

Putnis, A., Prieto, M., & Fernandez-Diaz, L. (1995) Fluid supersaturation and crystallization in porous media. Geological Magazine 132: 1–13.

Roedder, E., 1984, Fluid inclusions: Mineralogical Society of America, Reviews in Mineralogy 12, 644p.

Rost, D., Stephan, T., Greshake, A., Fritz, J., Weber, I., Jessberger, E. K., & Stöffler, D. (2009) A combined ToF-SIMS and EMP/SEM study of a three-phase symplectite in the Los Angeles basaltic shergottite. Meteoritics and Planetary Science 44: 1225–1237.

Sawyer, E.W., 2008, Atlas of migmatites: Quebec, Mineralogical Association of Canada, Canadian Mineralogist Special Publication 9, 386p.

Schiano, P. (2003) Primitive mantle magmas recorded as silicate melt inclusions in igneous minerals. Earth-Science Reviews 63: 121-144.

Sobolev, V.S. & Kostyuk, V.P. (1975) Magmatic crystallization based on a study of melt inclusions. Fluid Inclusions Research 9: 182-253 (translated from original publication in Russian).

Sorby, H.C. (1858) On the microscopical structure of crystals, indicating origin of minerals and rocks. Quarterly Journal of the Geological Society of London 14: 453–500.

Thomas, R., Kamenetsky, V.S. & Davidson, P. (2006) Laser Raman spectroscopic measurements of water in unexposed glass inclusions. American Mineralogist 91: 467-470.

Thomas, J.B., Bodnar, R.J., Shimizu, N. & Sinha, A.K. (2002) Determination of zircon/melt trace element partition coefficients from SIMS analysis of melt inclusions in zircon. Geochimica et Cosmochimica Acta 66: 2887–2901.

Thomas, R., Kamenetsky, V.S. & Davidson, P. (2006) Laser Raman spectroscopic measurements of water in unexposed glass inclusions. American Mineralogist 91: 467-470

Vernon, R.H. (1999) Quartz and feldspar microstructures in metamorphic rocks. Canadian Mineralogist 37: 513-524.

Vernon, R.H. (2004) A practical guide to rock microstructure. Cambridge, Cambridge University Press, 594 p.

Vernon, R.H. (2007) Problems in identifying restite in S-type granites of southeastern Australia, with speculations on sources of magma and enclaves. Canadian Mineralogist 45: 147-178.

Vernon, R.H. (2010) Granites Really Are Magmatic: Using Structural Evidence to Refute Some Obstinate Hypotheses. In: Marnie A. Forster, John D. FitzGerald & Gordon S. Lister (Eds.), The Science of Microstructure, 2010. Journal of the Virtual Explorer 35, paper 1, 10.3809/jvirtex.2010.00264

Vernon, R.H. (2011) Microstructures of melt-bearing regional metamorphic rocks, in van Reenen, D.D., Kramers, J.D., McCourt, S., & Perchuk, L.L. (eds.): Origin and Evolution of Precambrian High-Grade Gneiss Terranes, with Special Emphasis on the Limpopo Complex of Southern Africa. Geological Society of America Memoir 207: 1–XXX, 10.1130/2011.1207(01)

Vielzeuf, D. & Holloway, J.R. (1988) Experimental determination of the fluid-absent melting relations in the pelitic system. Contributions to Mineralogy and Petrology 98: 257-276.

Webster, J.D. (2006) Melt inclusions in plutonic rocks. Short Course Series, 36. Mineralogical Association of Canada, Quebec, 237 p.

Yang, K. & Bodnar, R.J. (1994) Why is economic porphyry copper mineralization absent from the granitoids of the Gyeongsang Basin, South Korea?: Evidence from silicate melt and aqueous fluid inclusions. International Geology Review 36: 608-628.

A. Table 1

Table 1. Mean electron microprobe and laser ablation ICP-MS analyses of glasses from El Hoyazo enclaves (SE Spain), the Kerala (S India) and Ronda (S Spain) migmatites, and some melting experiments from the literature.

Ocur-rence	**Enclave**	**Enclave**	**Enclave**	**Enclave**	**Enclave**	**Migm KKB**	**Migm KKB**	**Exp melt**	**Migm Ronda**	**Migm Ronda**
Micro-structure	MI in Pl	MI in Grt	MI in Crd	MI in Ilm	Matrix Gl	Nanogr MI	Glassy MI		Nanogr MI	Glassy MI
Electron microprobe analyses (concentrations in wt%)										
No. analyses	145	43	51	18	48	37[a]	7	1[b]	10[c]	3
SiO_2	72.90	71.51	73.56	70.68	70.60	73.08	75.41	72.28	70.01	69.69
TiO_2	0.08	0.10	0.07	0.31	0.17	0.08	0.11	0.39	0.07	0.08
Al_2O_3	12.87	14.45	14.07	15.69	13.99	13.31	12.09	13.75	11.30	11.78
FeO*	1.14	1.66	1.28	2.58	1.55	3.03	1.58	3.80	1.59	1.20
MnO	0.01	0.07	0.04	0.07	0.01	0.03	0.03	0.00	0.11	0.09
MgO	0.15	0.04	0.04	0.13	0.14	0.76	0.25	0.55	0.13	0.07
CaO	0.22	0.60	0.94	0.96	0.36	0.60	0.08	0.69	0.43	0.39
Na_2O	2.86	3.62	3.41	3.55	2.96	1.14	0.62	0.81	2.52	3.09
K_2O	5.10	4.92	4.87	4.92	5.54	6.76	7.73	7.73	3.95	4.19
P_2O_5	0.19	0.34	0.20	0.31	0.29	0.09	0.04	n.d	0.33	0.18
F	0.06	0.07	0.05	0.07	0.06	n.d.	n.d.	n.d.	n.d.	n.d.
Cl	0.01	0.01	0.45	0.00	0.01	0.25	n.d.	n.d.	n.d.	n.d.
O=F	-0.02	-0.03	-0.02	-0.03	-0.02					
O=Cl	0.00	0.00	-0.10	0.00	0.00	-0.05				
H_2O**	4.42	2.61	1.10	0.82	4.32	0.82	2.06	0.00	9.56	9.24
ASI	1.22	1.17	1.12	1.22	1.22	1.30	1.27	1.25	1.23	1.15
#K	0.54	0.47	0.48	0.48	0.55	0.79	0.89	0.86	0.51	0.47
#Mg	0.19	0.04	0.04	0.08	0.13	0.30	0.15	0.20	0.12	0.09
Laser ablation ICP-MS analyses (concentrations in ppm)										
No. analyses	18 to 22	8 to 12	4	3	20 to 28					
Rb	212	237	250	206	211	n.d.	n.d.	n.d.	n.d.	n.d.
Sr	28	112	135	242	82	n.d.	n.d.	n.d.	n.d.	n.d.
Ba	80	235	543	512	355	n.d.	n.d.	n.d.	n.d.	n.d.
V	0.72	0.16	2.0	9.7	2.3	n.d.	n.d.	n.d.	n.d.	n.d.
Zr	24	28	7.7	34	37	n.d.	n.d.	n.d.	n.d.	n.d.

Ocur-rence	Enclave	Enclave	Enclave	Enclave	Enclave	Migm KKB	Migm KKB	Exp melt	Migm Ronda	Migm Ronda
Th	1.53	1.1	0.83	3.3	3.5	n.d.	n.d.	n.d.	n.d.	n.d.
U	4.0	4.2	3.9	20	2.9	n.d.	n.d.	n.d.	n.d.	n.d.
Sum REE	18	21	35	69	44	n.d.	n.d.	n.d.	n.d.	n.d.
Eu/Eu*	0.69	2.5	1.2	1.2	1.4	n.d.	n.d.	n.d.	n.d.	n.d.
$(La/Lu)_N$	11	32	4.6	2.2	13	n.d.	n.d.	n.d.	n.d.	n.d.
* Total Fe as FeO										
** 100-total										
a Remelted at ~ 1040 °C with HT stage										
b From Droop *et al.* 2003										
c Remelted at 700 °C, 5 kbar with piston cylinder										
#K=mol. $K_2O/(K_2O+Na_2O)$										
#Mg=mol. MgO/(MgO+FeO*)										
Sum REE refers to total rare earth element concentration, and Eu/Eu* to the Europium anomaly										
$(La/Lu)_N$ refers to the ratio Lanthanum/Lutetium, normalized to the chondritic values										